

# Thermophysical Properties of Titanium Aluminides

Iván Egry<sup>1</sup>, Rob Brooks<sup>2</sup>, Dirk Holland-Moritz<sup>1</sup>, Rada Novakovic<sup>3</sup>, Taishi Matsushita<sup>4</sup>, Enrica Ricci<sup>3</sup>,  
Seshadri Seetharaman<sup>4</sup>, Rainer Wunderlich<sup>5</sup>

<sup>1</sup> German Aerospace Center, Cologne, Germany

<sup>2</sup> National Physical Laboratory, Teddington, UK

<sup>3</sup> Institute for Energetics and Interfaces, Genova, Italy

<sup>4</sup> Royal Institute of Technology, Stockholm, Sweden

<sup>5</sup> University of Ulm, Ulm, Germany

Titanium aluminides are an important class of materials for high temperature applications, e.g. for turbine blades. For the casting of such components, a precise knowledge of the thermophysical properties, both in the solid and in the liquid phase, is a crucial prerequisite. In the European Integrated Project IMPRESS, a central task is the measurement of the relevant thermophysical properties of the selected Ti-Al alloys. The properties to be measured comprise caloric data like heat of fusion, specific heat, thermal conductivity, as well as thermophysical and transport properties like density, surface tension and viscosity. In addition to conventional high-temperature equipment, also containerless methods are used. This paper discusses the results obtained so far.

**Keywords:** thermophysical properties, titanium aluminides, liquid metals, specific heat, density, surface tension, diffusivity, resistivity

## 1 Introduction

IMPRESS is an acronym for Intermetallic Materials Processing in Relation to Earth and Space Solidification<sup>1)</sup>. The main scientific objective of IMPRESS is to gain a better understanding of the links between materials processing routes, structure and final properties of intermetallic alloys. Technically speaking, the project aims to develop and test two distinct prototypes based on intermetallic materials; namely:

- 40 cm cast  $\gamma$ -TiAl turbine blades for aero-engines and stationary gas turbines
- < 20  $\mu\text{m}$ -sized Raney-type Ni-Al catalytic powder for use in hydrogen fuel cell electrodes and hydrogenation reactions.

Within the IMPRESS project, the measurement of thermophysical properties plays a central role, linking the experimental work and the modelling. The main tasks were to first define a measurement plan and then to experimentally determine a set of thermophysical data for high temperature melts of the selected TiAl / NiAl-based alloys. This set includes density, thermal expansion, enthalpy, specific heat, thermal diffusivity, electrical resistivity, and surface tension.

At the beginning of the IMPRESS project, the exact composition of the  $\gamma$ -Ti-Al was defined. The challenge was to develop a castable alloy, free of grain refiners, like boron, and susceptible to heat treatment. Finally, a ternary Ti-Al-Nb alloy was chosen, which is the subject of thermophysical property measurements reported here. The nominal composition is as follows:  $\text{Al}_{45.5}\text{Ti}_{46.5}\text{Nb}_8$  (at%). Data on the Raney-type Ni-Al catalytic materials are not shown here.

## 2 Measurements

### 2.1 DSC Measurements

Thermal analysis was performed in a high temperature differential scanning calorimeter (HTDSC) (Netzsch

Jupiter STA 449) with a maximum furnace temperature of 1923 K.

Calorimetry in the two phase region and in the liquid phase up to temperatures of  $T = 1883$  K is complicated by the high chemical reactivity of TiAlNb affecting enthalpy measurements, and - due to possible changes in the composition - the observed transition temperatures. Experiments were performed in Pt-cups with  $\text{Y}_2\text{O}_3$ -coated alumina inlays. This combination showed the least reaction between the specimen and the container.

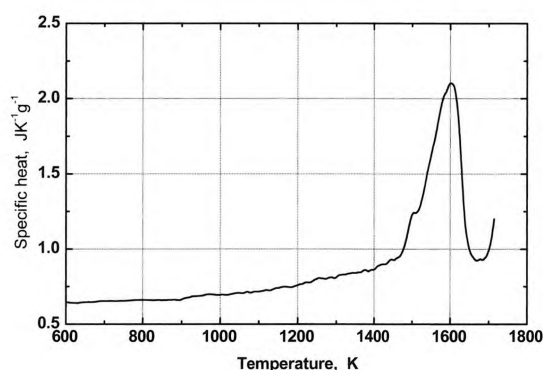


**Figure 1.** Specific heat capacity in the solid phase of  $\text{Al}_{45.5}\text{Ti}_{46.5}\text{Nb}_8$ .

The specific heat capacity in the solid phase from  $T = 600$  to  $1700$  K of TiAlNb, is shown in Figure 1. The temperature calibration is obtained from the iron  $\alpha \rightarrow \gamma$  and  $\gamma \rightarrow \delta$  phase transitions at  $T = 1184$  K and  $T = 1667$  K, respectively. The endothermic event in the TiAlNb thermogram with onset at  $T = 1468$  to  $1674^\circ$  K is identified with the  $\alpha_2 + \gamma \rightarrow \alpha + \gamma$  phase transition. The corresponding enthalpy is  $\Delta H_{\text{tr}} = 109.2$  (Jmol<sup>-1</sup>). Values of the onset of melting, and of the enthalpy of fusion were determined as follows:

$$T_s = 1773 \pm 5 \text{ (K)}, \quad \Delta H_f = 340.2 \pm 3 \text{ (J mol}^{-1}\text{)} \quad (1)$$

The value of the enthalpy of fusion obtained in this work is different from the value of  $\Delta H_f = 411.5 \text{ (Jg}^{-1}\text{)}$  obtained by rapid heating techniques<sup>2)</sup> for a  $\text{Ti}_{47}\text{Al}_{44}\text{Nb}_8\text{B}_1$  alloy. Heating rate dependent measurements have been performed to identify the equilibrium liquidus temperature. From extrapolating the values shown in Figure 2 to zero heating rate, a value of  $T_l = 1846 \pm 5 \text{ (K)}$  is obtained.

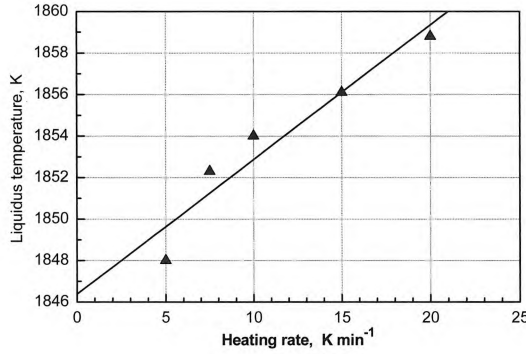


**Figure 2.** Apparent liquidus temperature of  $\text{Al}_{45.5}\text{Ti}_{46.5}\text{Nb}_8$ -alloy as a function of heating rate.

## 2.2 Laser Flash Measurements

The thermal diffusivity measurements were carried out as a round-robin exercise between NPL and KTH. Both labs used the Laser-Flash method (NPL: Netzsch 475, KTH: Shinku-Riko, TC-7000H/MELT). The heating and cooling rate was 10 and 6 K/min, respectively. The thermal diffusivity was measured in the solid phase from room temperature to 1600 (K) on heating and cooling, and is shown in Figure 3. Squares represent the measurement results at KTH, while circles correspond to data obtained by NPL. All results are fitted by a third order polynomial, and the average between heating and cooling is taken as the recommended value:

$$\alpha = 3.754 + 0.00516 T + 1.89 \cdot 10^{-6} T^2 - 2.69 \cdot 10^{-9} T^3 \quad (10^{-6} \text{ m}^2 \text{ s}^{-1}) \quad (300 \text{ K} < T < 1600 \text{ K}) \quad (2)$$

## 2.3 Density

Thermal expansion measurements were carried out from room temperature to 1600 (K) using a Linseis dilato-meter. The first run showed a difference between heating and cooling behaviour which is likely to be the effect of annealing the sample. Two further runs were carried out on the same sample, and the agreement between heating and cooling in these cases was far better, indicating a fully annealed specimen. The data show a minor change in slope at about 1000 (K), which can also be found in the electrical resistivity data, and is marked in the thermal diffusivity data at 1100 (K). A more noticeable deviation occurs at 1500 (K), which is also seen in the electrical resistivity values. This is likely to be associated with phase changes, although detailed metallography has not been carried out on specimens quenched from these tempe-

ratures. The density of the solid alloy is determined from the room temperature density and the thermal expansion and is shown in Figure 4.

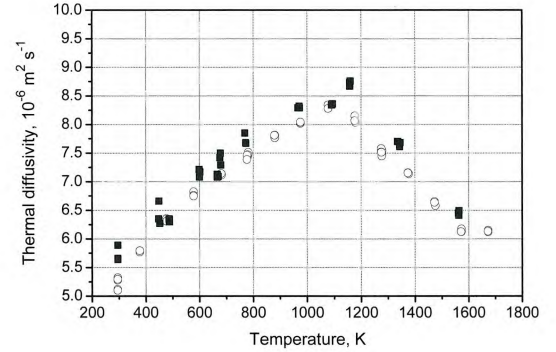


**Figure 3.** Thermal diffusivity of  $\text{Al}_{45.5}\text{Ti}_{46.5}\text{Nb}_8$  alloy

The density of stable and deeply undercooled melts has been investigated by the levitated drop method. The temperature of the samples is contactlessly measured with a single-colour pyrometer. In order to determine the density of the melt, the samples were illuminated by a He-Ne laser beam and the shadowgraph of the sample was recorded by use of a CCD camera. Under the assumption that the shape of the specimen is axially symmetric, the density of the melt is inferred from the edge profile of the shadowgraph. The experimental setup and the data evaluation procedure is described in detail elsewhere<sup>3)</sup>. The results of the investigations obtained for two different samples are shown in Figure 5. A broad temperature range is covered ranging from 1585 to 1940 (K) ( $T_L = 1846 \text{ K}$ ).

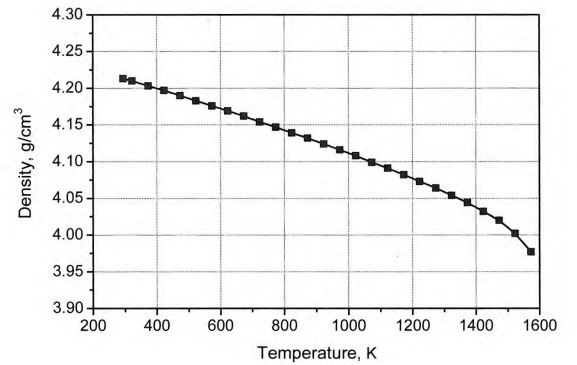


**Figure 4.** Density of solid  $\text{Al}_{45.5}\text{Ti}_{46.5}\text{Nb}_8$  alloy.

The temperature dependence of the density of the liquid  $\text{TiAlNb}$  alloy is described by the following linear fit:

$$\rho = 3.85 - 4.57 \cdot 10^{-4} (T - T_L) \text{ (g cm}^{-3}\text{)} \quad (3)$$

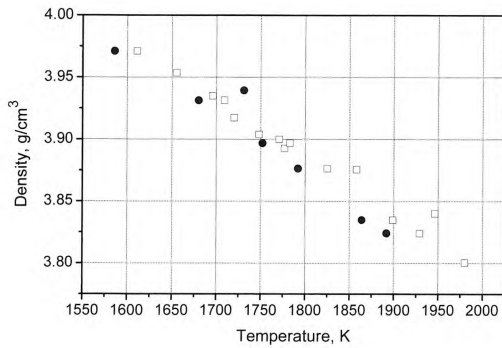


**Figure 5.** Density of liquid  $\text{Al}_{45.5}\text{Ti}_{46.5}\text{Nb}_8$ - as a function of the temperature.

## 2.4 Surface Tension

The surface tension of stable and undercooled TiAlNb melts is measured by use of the same electromagnetic levitation device that was also utilized for the density measurements described above. For determination of the surface tension the oscillating droplet method<sup>4)</sup> is applied. The oscillations of the sample surface are recorded from the top of the levitator with a video camera at a frame rate of 400 Hz with a pixel resolution of 1024x1000 pixels. At each investigated temperature a series of 4096 frames is acquired.

From the video sequences frequency spectra of the sample radius,  $R$ , are determined. The spectrum contains five peaks at frequencies  $\omega_i$  ( $i = -2, -1, 0, 1, 2$ ) resulting from the surface oscillations. Moreover, three translational frequencies  $T_x$ ,  $T_y$  and  $T_z$  can be identified.

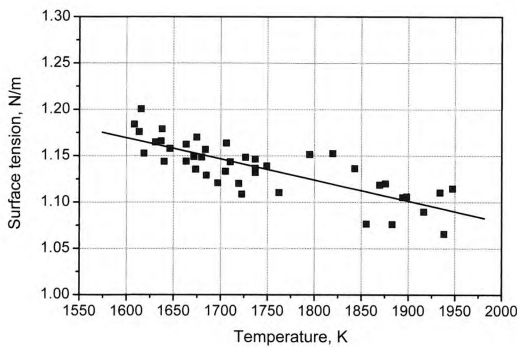


**Figure 6.** Surface tension of liquid  $\text{Al}_{45.5}\text{Ti}_{46.5}\text{Nb}_8$ - as a function of the temperature. The line is a linear fit to the data.

From the five surface oscillation frequencies and the three translational frequencies the surface tension,  $\gamma$ , is determined by use of the formula by Cummings and Blackburn<sup>5)</sup> :

$$\gamma = \frac{3M}{160\pi} \sum_{m=-2}^2 \omega_i^2 - 1.9 \cdot \Omega^2 - 0.3 \cdot \left(\frac{g}{a}\right)^2 \Omega^{-2} \quad (4)$$

$$\text{with } \Omega^2 = \frac{1}{3}(T_x^2 + T_y^2 + T_z^2) \quad (5)$$

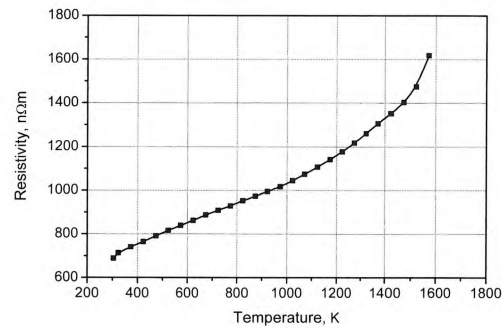
Here  $M$  denotes the sample mass.

Figure 6 shows the measured surface tension as a function of the temperature. Its temperature dependence is described by the following linear fit

$$\gamma = 1.114 - 2.17 \cdot 10^{-4} (T - T_L) \text{ (N m}^{-1}\text{)} \quad (6)$$

## 2.5 Electrical Resistivity

Electrical resistivity measurements of solid TiAlNb were carried out in an ETMT apparatus. The sample is heated by a DC current and via two thermocouple wires, welded to the sample, a four probe resistance measurement is taken. The heating rate is 5°C per second. An initial resistance measurement is made at room temperature. The results are given in Figure 7.



**Figure 7.** Electrical resistivity of two different solid  $\text{Al}_{45.5}\text{Ti}_{46.5}\text{Nb}_8$ - samples.

A slight deviation from linearity is seen between 943 and 1013 (K), and a larger deviation at 1464 to 1475 (K). The change at the lower temperature may be attributable to a minor phase change in the material, as it is also seen in the thermal expansion and thermal diffusivity data. However the temperatures at which it is observed vary from specimen to specimen. The high temperature deviation is more reproducible. The measurements ended when the platinum thermocouple wires (Pt/Pt+13%Rh) detached from the sample. This was caused by the melting of the wire as it reacted to form a Ti-Pt eutectic. The onset of this process can be seen at the highest temperatures of the tests where the resistivity values drop as a liquid begins to form.

## 2.6 Thermodynamic Modelling

In order to understand better the mixing properties of the TiAlNb alloy system, particular attention was dedicated to the Al-Ti system and to the effect of a third component, Nb, on it. The thermophysical properties of the binary Al-Ti liquid alloy system have been investigated by a simple structural model for chemical complexes (CFM)<sup>6)</sup> as well as by the Quasi-Chemical Approximation

(QCA)<sup>7)</sup> for a regular solution. In this way, the effect of short range order phenomena on the surface properties of Al-Ti liquid alloys can be estimated from the difference in surface composition or surface tension calculated by the two models. Available experimental data on the thermodynamic properties as well as phase diagram information have been used for the calculation of order energy parameters for the liquid phase in the Al-Ti system. For all temperatures the mixing functions, i. e. the Gibbs free energy of mixing and enthalpy are negative and exhibit flat minima near the mole fraction  $c_{Ti} = 0.43$ . The AlTi intermetallic phase was postulated as energetically favoured and the preferential arrangements of Al and Ti constituent atoms favour the formation of AlTi-complexes in the liquid alloys.

The optimized data set of the excess Gibbs energy of mixing of Al-Ti liquid alloys<sup>8)</sup> together with the Gibbs energy of mixing<sup>9)</sup>, the enthalpy of mixing<sup>10)</sup>, and activity data<sup>11),12)</sup>, have been used to calculate the CFM interaction energy parameters at  $T = 1973$  (K).

In the present work, the surface tensions of the pure components, Al and Ti, are taken from the literature<sup>13),14)</sup> Due to their affinity for oxygen, these values exhibit a large scatter. Therefore, it is important to notice that, for different choices of the surface tension reference data, the calculated values will be different.

The surface tensions of Al-Ti molten alloys at 1973 (K) are shown in Figure 8. For this temperature the surface tension isotherms have been calculated using the CFM, the QCA for regular solution, as well as the ideal solution model. As can be seen, both surface tension isotherms, calculated either by the CFM or the QCA for regular solution, deviate positively with respect to the ideal solution model, confirming that liquid alloys with negative excess Gibbs energy in the bulk exhibit positive surface tension deviations with respect to ideal behaviour. The clustering effects on the surface tension and surface segregation are antagonistic, and thus the surface tension isotherm obtained by the CFM is higher than that calculated by the QCA.

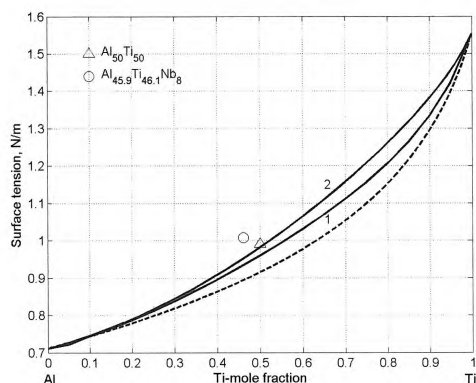


**Figure 8.** Surface tension of Al-Ti liquid alloys at  $T = 1973$  (K). (1 — QCA; 2 — CFM; - - - ideal solution). For comparison, the surface tension of the  $Al_{45.5}Ti_{46.5}Nb_8$  alloy is also shown.

Except for the surface tension of  $Al_{50}Ti_{50}$ , there is a complete lack of experimental data. It is worth noting that this result agrees very well with the corresponding CFM-calculated value.

In order to estimate the effects of a third component on the surface tension, the experimental result on the  $Ti_{46.1}Al_{45.9}Nb_8$  is also shown. Assuming the Ti-content as constant, at  $T = 1973$  (K), the surface tension of this alloy is higher with respect to the Al-50%Ti due to the contribution of Nb.

### 3 Summary

Within the IMPRESS project, a concerted action was taken to determine the thermophysical properties of an  $Al_{45.5}Ti_{46.5}Nb_8$  alloy, suitable for casting large turbine blades. Whereas conventional methods worked up to 1573 (K) in the solid phase, difficulties were encountered to process the liquid phase in a crucible. This prevented the measurements of specific heat, viscosity and electrical conductivity in the liquid phase. Density and surface tension of liquid TiAlNb were measured using electromagnetic levitation as a containerless technique. The data obtained are used for subsequent simulation of the casting process.

### Acknowledgement

This work was carried out under contract FP6-500635-2 of the European Commission.

### REFERENCES

- 1) D. Jarvis, Materials Word, 2005, 11
- 2) R. Harding, R. Brooks, G. Pottlacher, J. Brillo, *Gamma Titanium Aluminides*, Y. Kim, H. Clemens, A. Rosenberger eds., TMS, 2003, 75
- 3) J. Brillo and I. Egry, Int. J. Thermophys. 24, 1155 (2003).
- 4) D.M. Herlach, R.F. Cochrane, I. Egry, H.J. Fecht, A.L. Greer, Int. Mater. Rev. **38**, 273 (1993)
- 5) D.L. Cummings and D.A. Blackburn, J. Fluid Mech. **224**, 395 (1991).
- 6) A.B. Bhatia, R.N. Singh, Phys. Chem. Liq. 13 (1984) 177
- 7) R.N. Singh, Can. J. Phys. 65 (1987) 309.
- 8) F. Zhang, S.L. Chen, Y.A. Chang, U.R. Kattner, Intermetallics 5 (1997) 472
- 9) F. Zhang, W. Huang, Y.A. Chang, Calphad 21(3) (1997) 337
- 10) Yu.O. Esin, N.P. Bobrov, M.S. Petrushevskii, P.V. Gel'd, Russian Metallurgy 5 (1974) 86
- 11) M. Maeda, T. Kiwaki, K. Shibuya, T. Ikeda, Mater. Sci. and Eng. A239-240 (1997) 276
- 12) N.S. Jacobson, M.P. Brady, G.M. Mehrotra, Oxidation of Metals, 52(516) (1999) 537
- 13) G. Lang, P. Laty, J.C. Joud, P. Desré, Z. Metallkde, 68(2) 1977 113
- 14) T. Ishikawa, P.-F. Paradis, T. Itami, S. Yoda, J. Chem. Phys. 118(17) (2003) 7912